

Published in final edited form as:

J Med Chem. 2005 March 24; 48(6): 1849–1856.

Discovery of a Potent, Selective, and Efficacious Class of Reversible α -Ketoheterocycle Inhibitors of Fatty Acid Amide Hydrolase Effective as Analgesics^a

Dale L. Boger^{†,§,*}, Hiroshi Miyauchi^{†,§}, Wu Du^{†,§}, Christophe Hardouin^{†,§}, Robert A. Fecik^{†,§}, Heng Cheng^{†,§}, Inkyu Hwang^{†,§}, Michael P. Hedrick^{†,§}, Donmienne Leung^{‡,§}, Orlando Acevedo^{||}, Cristiano R. W. Guimarães^{||}, William L. Jorgensen^{||}, and Benjamin F. Cravatt^{†,§}

[†]Department of Chemistry, The Scripps Research Institute, 10550 North Torrey Pines Road, La Jolla, California 92037

[‡]Department of Cell Biology, The Scripps Research Institute, 10550 North Torrey Pines Road, La Jolla, California 92037

[§]The Skaggs Institute for Chemical Biology, The Scripps Research Institute, 10550 North Torrey Pines Road, La Jolla, California 92037

^{||}Department of Chemistry, Yale University, 225 Prospect St., New Haven, Connecticut 06520-8107

Abstract

Fatty acid amide hydrolase (FAAH) degrades neuromodulating fatty acid amides including anandamide (endogenous cannabinoid agonist) and oleamide (sleep-inducing lipid) at their sites of action and is intimately involved in their regulation. Herein we report the discovery of a potent, selective, and efficacious class of reversible FAAH inhibitors that produce analgesia in animal models validating a new therapeutic target for pain intervention. Key to the useful inhibitor discovery was the routine implementation of a proteomics-wide selectivity screen against all serine hydrolases ensuring selectivity for FAAH coupled with systematic in vivo examinations of candidate inhibitors.

Introduction

Anandamide (**1a**)¹ and oleamide (**1b**)^{2–4} have emerged as the prototypical members of a class of endogenous fatty acid amides that serve as chemical messengers. Anandamide, the most recognizable member of the endogenous fatty acid ethanolamides,⁵ binds and activates the central (CB1) and peripheral (CB2) cannabinoid receptors through which it is thought to exert its biological effects. More recently, **1a** was shown to activate the vanilloid receptor (VR1) analogous to capsaicin and olvanil (*N*-vanillyloleamide) providing an additional site of action that may contribute to its analgesic effects and an intriguing structural–functional relationship with oleamide.^{9,10} Anandamide, like the cannabinoids, exhibits a range of biological properties that includes not only behavioral analgesia suppressing pain neurotransmission,¹¹ but also anxiolytic, antiemetic, appetite enhancement, and antiproliferative activity as well as neuroprotective effects that have clinical implications in the treatment of sleep disorders, anxiety, epilepsy, cachexia, cancer, and neurodegenerative disorders.^{6–8}

^aIn memory of Dr. Paul Janssen, his warm friendship, and his lasting impact on Medicinal Chemistry.

*corresponding author Dale L. Boger, Department of Chemistry, The Scripps Research Institute, 10550 North Torrey Pines Road, La Jolla, CA 92037, Phone: 858-784-7522, Fax: 858-784-7550, E-mail: boger@scripps.edu.

Oleamide was found to accumulate in the cerebrospinal fluid under conditions of sleep deprivation. In a dose-dependent manner, it was found to induce physiological sleep in animals where it reduced mobility, shortened the sleep induction period, and lengthened the time spent in slow wave sleep 2 at the expense of waking.^{2,12} In addition to suggesting that oleamide may play a central role in sleep, the studies indicate the potential of developing sleep aids that lack the side effects of sedatives and hypnotics and the suicide-abuse potential of such central nervous system (CNS) depressants.

Fatty acid amide hydrolase (FAAH)¹³⁻¹⁵ is an integral membrane protein that degrades fatty acid primary amides and ethanolamides including anandamide and oleamide, Figure 1.^{16,17} Its CNS distribution indicates that it degrades neuromodulating fatty acid amides at their sites of action and is intimately involved in their regulation.¹⁸ FAAH constitutes the only known mammalian member of the class of amidase enzymes that all bear a unique catalytic mechanism (Ser-Ser-Lys triad).^{15,19-22} Significantly, FAAH knockout mice not only proved healthy indicating no untoward consequences attributable to the lack of enzyme, but they also exhibited greatly augmented behavioral responses to administered anandamide²³ and oleamide²⁴ and increased endogenous brain levels of fatty acid amides that correlated with a CB1-dependent analgesic phenotype.^{23,25} As a result of its unique mammalian distribution, its selectively targetable active site and catalytic mechanism, and the consequences of its inhibition (increased endogenous levels of anandamide and oleamide), FAAH has emerged as a potentially exciting new therapeutic target for a range of clinical disorders.²⁶⁻²⁸

Despite this interest, few FAAH inhibitors have been disclosed.²⁹⁻⁴¹ These include the discovery that the endogenous sleep-inducing compound 2-octyl α -bromoacetoacetate is an effective FAAH inhibitor,²⁹ a series of reversible inhibitors bearing nonselective electrophilic carbonyls³⁰⁻³² (e.g., trifluoromethyl ketones), and a set of irreversible inhibitors³³⁻³⁷ (sulfonyl fluorides or fluorophosphonates). Recently, two classes of inhibitors have been disclosed that promise to advance the potential of FAAH as a therapeutic target.³⁸⁻⁴¹ The most recent is a class of aryl carbamates that acylate an active site catalytic Ser and which were shown to exhibit anxiolytic activity in animal models.^{38,39} The second is an earlier class of α -ketoheterocycle-based inhibitors that possess extraordinary potency (K_i = 100–200 pM) and that act as reversible, competitive inhibitors presumably via reversible hemiketal formation with an active site Ser.^{40,41}

Herein we report the discovery of a class of potent, selective, and efficacious inhibitors of FAAH that produce analgesia in animal models providing the first validation of this new therapeutic target for the treatment of pain disorders which emerged from our continued investigations of such α -ketoheterocycles. Key to the useful inhibitor discovery was the implementation of a proteomics-wide selectivity screen against all serine hydrolases⁴² ensuring selectivity for FAAH coupled with systematic in vivo examinations of candidate inhibitors.⁴³

Inhibitor Synthesis

The candidate inhibitors were prepared by direct acid chloride acylation of a Zn/Cu metalated oxazole following the protocol of Anderson et. al.⁴⁴ (Scheme 1a), selected instances of direct oxazole lithiation and reaction with a Weinreb amide⁴⁵ (Scheme 1b), or Stille coupling⁴⁶ of a 5-iodo- or 5-tributylstannyloxazole followed by TBS ether deprotection and Dess–Martin periodinane oxidation (Scheme 1c).⁴⁷ In turn, the 5-iodo- or 5-tributylstannyloxazoles were obtained by the Vedejs oxazole metalation⁴⁸ and aldehyde condensation, TBS protection of the alcohol, followed by a selective C5-oxazole lithiation⁴⁹ and subsequent reaction with I_2 or Bu_3SnCl .

Inhibition Studies

Enzyme assays were performed at 20–23 °C with purified recombinant rat FAAH expressed in *E. coli*⁵⁰ (unless indicated otherwise) or with solubilized COS-7 membrane extracts from cells transiently transfected with human FAAH cDNA¹⁴ (where specifically indicated) in a 125 mM Tris/1 mM EDTA/0.2% glycerol/0.02% Triton X-100/0.4 mM Hepes, pH 9.0 buffer.²⁹ The initial rates of hydrolysis (≤ 10 –20% reaction) were monitored using enzyme concentrations at least 3 times below the measured K_i by following the breakdown of ¹⁴C-oleamide and K_i 's established as described (Dixon plot).⁴⁰ Lineweaver–Burk analysis established reversible, competitive inhibition (Figure 2).

Results and Discussion

In initial studies,⁴⁰ a series of candidate α -ketoheterocycle inhibitors were examined that incorporated the oleyl side chain. Of these, benzoxazole **2** was selected for detailed examination since it was amenable to systematic exploration (Figure 3). Its modification to the oxazolopyridine **3** with incorporation of an additional basic nitrogen resulted in a remarkable 100-fold increase in inhibitor potency. Although this increase in potency was greatest with **3**, it was not limited to a single positional isomer and each variant on the oxazolopyridine structure exhibited 50–200 fold increases in K_i over **2**. Systematic modification of the fatty acid side chain provided the exceptionally potent FAAH inhibitors **4–7**.

Substituted α -Keto Oxazoles

An additional promising α -ketoheterocycle disclosed in these initial studies was oxazole **9a** (Table 1).⁴⁰ We subsequently found that 4,5-disubstitution of **9a** with two alkyl or phenyl substituents diminished (**9b**) or abolished (**9c**) activity, but a single 4- or 5-phenyl substituent (**9d** and **9e**) led to only small reductions in potency with each exhibiting K_i 's comparable with benzoxazole **2**. Consequently, a series of 4- and 5-substituted oleyl α -keto oxazoles bearing each pyridine positional isomer was examined (Table 1). Analogous to observations made with the oxazolopyridines (e.g. **3**), each exhibited 5–20 fold increases in K_i over **9d** or **9e**. Thus, incorporation of an additional weakly basic nitrogen proximal to the oxazole substantially increased FAAH inhibition. Although each isomer exhibited this increase, it was most pronounced with **9f** and **9g** mirroring the pattern observed with the oxazolopyridines.⁴⁰ C5-substitution of the oxazole with alternative six-membered heterocycles bearing two or more weakly basic nitrogens (**9l–o**), one of which overlays with 2-pyridyl nitrogen of **9f**, provided potent FAAH inhibitors with activity indistinguishable from **9f**.

A revealing set of oxazoles was examined that were substituted at C5 with a rationally chosen series of five-membered heteroaromatics (**9p–w**). The inhibitor potency smoothly increased as the H-bond acceptor capabilities of the heteroaromatic substituent increased (N-methylpyrrole < thiophene < furan < N-methylimidazole < thiazole (= pyridine **9f**) < oxazole). Notably, the 5-(2-thiazolyl) derivative **9t** proved equally potent with **9f**, while the 5-(2-oxazolyl) derivative **9u** was slightly more potent. Mirroring the pattern observed with the pyridyl substituents (**9f–9k**), the derivatives where the H-bond acceptor is located adjacent to the oxazole linkage site (e.g. 2-furyl) were >10-fold more potent than the positional isomers (e.g. 3-furyl, **9q** vs **9v** and **9r** vs **9w**).

The Fatty Acid Chain

Enlisting the 5-(2-pyridyl)oxazole-2-yl heterocycle identified with **9f**, well-behaved trends were observed with modifications in the fatty acid chain (Table 2). The greatest potency was observed with saturated straight chain lengths of C10–C12 that corresponds to the location of the $\Delta^{9,10}$ double bond of oleamide and the $\Delta^{8,9/\Delta^{11,12}}$ double bonds of anandamide. This

corresponds to the location of a bend in the inhibitor bound conformation that was identified in our early inhibitor studies³² and confirmed in a FAAH x-ray structure.²² The potency for **10a–n** increased as the chain length was shortened from C18 to C12 (K_i , 60 → 2 nM), leveled off at C12–C10 (K_i , 2–9 nM), and diminished smoothly as the chain length was progressively shortened (K_i , 2 → >100,000 nM). Thus, each of first C1–C12 carbons contributes progressively to inhibitor binding affinity, whereas C14–C18 of the longer inhibitors progressively reduce potency.^{32,40}

Identical trends were observed with the incorporation of a phenyl ring at the chain terminus. An optimal potency was observed with the linker length of C6 (**11f**, K_i 5 nM) corresponding to a C10/C12 full length chain, although comparable potencies were observed with C5–C9, and progressive declines in activity were seen as the chain length was increased or decreased from C6. Notably, the position of the phenyl π -system in **11f** corresponds to the location of the oleamide $\Delta^{9,10}$ double bond or the anandamide $\Delta^{8,9}/\Delta^{11,12}$ double bonds. Thus, well-defined parabolic relationships were observed with the inhibitor chain length culminating in optimal potencies with **10d** for the saturated straight chain inhibitors and with **11f** for the Ph(CH₂)_n series **11a–j**.

Analogous to prior observations,^{31,32,40} the C18 alkyne **12** (K_i 10 nM) was 2-fold more potent than the alkene **9f** bearing the oleyl side chain (K_i 18 nM) which in turn was 3-fold more potent than the saturated C18 inhibitor **10a** (K_i 59 nM). Although they are not among the most potent inhibitors in the series, the activity of alkyne **12** is notable, approaches that of **10d** and **11f**, and it emerged as an especially interesting candidate inhibitor in the selectivity screening.

α -Substitution

Consistent with past observations,⁴¹ α -methyl or α,α -dimethyl substitution of **9a** resulted in 10-fold and 100-fold reductions, respectively, in activity (Table 3).

Further Exploration of the Oxazole Heteroaromatic Substituent

With the emergence of **11f** as a selective FAAH inhibitor displaying efficacious in vivo activity,⁴³ a series of heteroaromatic substituents were examined including those first found to be potent in the oleyl series (cf. Table 1). Consistent with these observations, **20a** bearing a C5 phenyl substituent was 30-fold less active than **11f** and each derivative incorporating a six-membered heterocycle containing two basic nitrogens (one of which is placed to overlay the 2-pyridyl nitrogen of **11f**) matched (**20b**, **d** and **e**), or modestly exceeded (**20c**) the potency of **11f** (Table 4). Interestingly and like the observations made in Table 1, altering the position of the basic nitrogen on the attached heterocycle (**20f**, 3 vs 2 position) resulted in a 5–10 fold loss in inhibitory potency. Finally, a series of five-membered heteroaromatic substituents **20g–j** similarly provided effective FAAH inhibitors where the potency again smoothly increased as their H-bonding capabilities increased. Notably, both the 5-(2-thiazolyl) derivative **20i** and the 5-(2-oxazolyl) derivative **20j** matched the potency of **11f**.

The Electrophilic Carbonyl

Key to the inhibitor design is the electrophilic carbonyl and its reversible hemiketal formation with an active site Ser nucleophile. Confirming this behavior, a series of alcohol precursors to the α -keto oxazoles was examined and each was found to be approximately 1000 times less potent than the corresponding ketone (Table 5). Nonetheless, they approximate or exceed the activity of many of the early FAAH inhibitors^{29–32} and many of the original α -ketoheterocycles.⁴⁰ Moreover, in the two instances examined (**22** and **24**) where the hydroxyl group has been further removed, the methylene derivatives retain much of the activity of the corresponding alcohol. This behavior indicates that the 5-(2-pyridyl)oxazole contributes significantly to FAAH active site binding independent of the electrophilic carbonyl. As such,

the heterocycles serve not only to enhance the electrophilic character of the keto group facilitating trap of the active site Ser nucleophile as a stable hemiketal, but they also form substantial and selective stabilizing active site interactions that contribute significantly to the binding affinity.

Notably, the α -keto oxazoles examined herein do not exist predominantly in the hydrated (gem diol) state, rather they are isolated as the ketones. Moreover, NMR experiments conducted with **9f** and **11f** in CD₃OD, 7% D₂O–acetone-*d*₆, and 5% D₂O–DMSO-*d*₆ revealed less than 5% hemiacetal or gem diol formation. Under identical conditions, the oleyl trifluoromethyl ketone^{31,40} was completely (CD₃OD) or predominately hydrated (ca. 90%, 7% D₂O–acetone-*d*₆).

Inhibition of Recombinant Human FAAH

Rat and human FAAH are very homologous (84% sequence identity), exhibit near identical substrate selectivities and inhibitor sensitivities in studies disclosed to date,⁴⁰ and embody an identical amidase signature sequence suggesting the observations made with rat FAAH would be analogous to those made with the human enzyme. Consequently, key inhibitors in the series were examined against the human enzyme and found to exhibit the same relative and absolute potencies (Table 6).

Selectivity Screening

Early assessments of inhibitors in the α -ketoheterocycle series against candidate competitive enzymes (phospholipase A2, ceramidase) revealed no inhibition. In the absence of identifiable competitive enzyme targets (FAAH constitutes the only known mammalian amidase bearing the unusual Ser–Ser–Lys catalytic triad) and since the candidate inhibitors did not effect the obvious hydrolases that are known to act on fatty acid ester or amide substrates, a proteomics-wide screen capable of assessing all serine proteases applicable to defining the selectivity of FAAH inhibitors was developed.⁴² This permits the simultaneous assessment of all relevant competitive enzymes including those that might be unrecognized, lack known substrates, or are even presently unknown. Moreover, this competitive parallel profiling of the inhibitors against all proteome serine hydrolases requires no use of a competitive substrate, no modification of the candidate inhibitor, and can rapidly and quantitatively establish relative potency and selectivity factors for each inhibitor. Thus, the IC₅₀ values in the selectivity screen are typically higher than the measured *K*_i's, but the relative and absolute potency and rank order determined in the assay parallels that established by standard substrate assays.⁴² Only two enzymes emerged in our screens as competitive targets for the α -ketoheterocycles detailed herein: triacylglycerol hydrolase (TGH) and an uncharacterized membrane-associated hydrolase that lacks known substrates or function (KIAA1363).

Summarized in Table 7 are representative results of the selectivity screening that permitted a simultaneous optimization of selectivity for FAAH over the two competitive enzymes displaying distinct SAR (structure–activity relationship) profiles conducted concurrent with the FAAH inhibition optimization (multidimensional SAR). Simple electrophilic carbonyl-based inhibitors including trifluoromethyl ketones exhibit an intrinsic selectivity that typically favors TGH by >1000-fold and KIAA by 10–100 fold (Table 7). Despite this unfavorably intrinsic selectivity, the identification of inhibitors selective for FAAH over KIAA proved straightforward. The inhibitor potency for FAAH versus KIAA typically increases as the side chain size (length) increases thereby improving selectivity, and the affinity for KIAA is completely or substantially disrupted with the introduction of the electrophilic carbonyl heterocycle such that the FAAH selectivity is satisfactory or superb (>1000-fold where measurable) which we attribute simply to the increased active site steric requirements (size) of such inhibitors. Even more impressive given the intrinsic >1000-fold TGH selectivity, the

screening revealed that the inhibitor potency and selectivity for TGH decreases as the side chain size (length) increases, and that the incorporation of a properly positioned second weakly basic nitrogen (H-bond acceptor) into the electrophilic carbonyl heterocycle can improve FAAH affinity and selectivity over that of TGH. Moreover, the selectivity of the 5-(2-pyridyl) oxazol-2-yl heterocycles disclosed herein (FAAH > TGH > KIAA) exceeds that of the corresponding predecessor oxazolopyridines (e.g. **9f** vs **3**, **11f** vs **6** or **7**, and **12** vs **4**), which in turn exceed and overcome the intrinsic selectivity for TGH or KIAA observed with the simpler α -ketoheterocycles (e.g., **2** and **8**) or trifluoromethyl ketone inhibitors, and useful selectivities are achieved within simple structures, Table 7.

Model of Inhibitors Bound to FAAH: Key Interactions

MC simulations for the α -keto oxazole derivatives **9f** and **11f** covalently bound to the enzyme were performed. The average structure that emerged features an extensive hydrogen-bonded network between the enzyme and the pyridyl nitrogen and oxazolyl oxygen of the inhibitors. More specifically, the oxazolyl oxygen is hydrogen bonded to the hydroxyl group of Ser217 of the catalytic triad, which accepts a hydrogen bond from the protonated nitrogen of Lys142, also from the catalytic triad. The side chain of this residue donates hydrogen bonds to the pyridyl nitrogen of the inhibitors, and to the hydroxyl groups of Ser218 and Thr236. An additional hydrogen bond is formed between the pyridine nitrogen of both **9f** and **11f** and the hydroxyl group of Thr236. The central role of the pyridyl nitrogen in the network and, especially, its interactions with Lys142 are consistent with the large activity boost between **9d** and **9f**. The carbonyl group of the third member of the catalytic triad (Ser241) accepts hydrogen bonds from the hydroxyl group and backbone nitrogen of Ser218. The side chain oxygen of Ser241, covalently bound to the carbonyl group of the inhibitors, accepts a hydrogen bond from the hydrogen on nitrogen of Ser217. These interactions are depicted in Figure 4a for the **9f** derivative. A closer look at Figure 4a also suggests an explanation for the high activities for **9l**, **9n**, **20b**, **20c**, **20d**, and **20e**. Although they would have to pay a larger dehydration penalty due to additional interactions between the solvent and the pyridazine, pyrimidine, and pyrazine rings, the second nitrogen atoms may form additional hydrogen bonds with the thiol groups of Cys144 and Cys269.

Regarding the interactions for the oxyanion, the negatively charged oxygen of both **9f** and **11f** is hydrogen bonded to the backbone nitrogens of Ile238, Gly239, and Ser241 (Figure 4a). As for the lipid chain of the derivatives, the longer chain of **9f** is surrounded by a number of hydrophobic residues, such as Leu192, Phe194, Tyr335, Leu372, Ala377, Leu380, Phe381, Leu404, Phe432, Thr488, Ile491, Val495, and Trp531 (Figure 4b), while the shorter chain of **11f** makes contact with Leu192, Leu380, Leu404, Ile491, Thr488, and Phe194.

Conclusions

In recent studies, we showed that **11f** (OL-135) potentiates the effects of exogenously administered anandamide, increases the endogenous levels of fatty acid amides in the central nervous system, and produces CB1-dependent analgesia in multiple nociceptive models, validating FAAH as an important new therapeutic target for the management of pain.⁴³ Key to this development was the systematic optimization of FAAH inhibition concurrent with a proteome-wide screening for FAAH selectivity that distinguished the 5-(2-pyridyl)-2-oxazoles described herein from the predecessor α -ketoheterocycles.

Experimental

1-Oxo-1-[5-(2-pyridyl)oxazol-2-yl]-7-phenylheptane (11f)

A solution of 7-phenylheptanoic acid (1.20 g, 5.80 mmol) in 20 mL of anhydrous CH_2Cl_2 at 0 °C was treated $(\text{COCl})_2$ (1.8 mL, 20.6 mmol) and 15 μL of DMF. After 1 h, the solution was allowed to warm to 25 °C and was stirred for 2.5 h. Concentration provided the crude acid chloride that was used directly in the next step.

A solution of 5-(2-pyridyl)oxazole (680 mg, 4.65 mmol) in 25 mL of anhydrous THF was treated with *n*-BuLi (2.2 mL, 2.5 M in hexanes, 5.5 mmol) and stirred for 35 min at -78 °C. The mixture was allowed to warm at 0 °C and ZnCl_2 (11.2 mL, 0.5 M in THF, 5.6 mmol) was added dropwise over 20 min. After 45 min, CuI (1.05 g, 5.6 mmol) was added and the solution was stirred for 15 min at 0 °C. 7-Phenylheptanoyl chloride (5.80 mmol) in anhydrous THF and added dropwise. After 1 h, the reaction was quenched with the addition of saturated aqueous NaHCO_3 and the mixture was extracted with EtOAc. The organic layers were combined, dried (Na_2SO_4), and concentrated. Chromatography (SiO_2 , 4 × 10 cm, 20% EtOAc-hexanes) afforded **11f** as a yellow solid. Treatment with aqueous 2 N KOH, extraction with EtOAc followed by a wash with saturated aqueous NaCl provided **11f** (1.00 g, 65%) as a pale yellow crystalline powder: mp 45–48 °C; ^1H NMR (500 MHz, CDCl_3) δ 8.76–8.74 (m, 1H), 7.96–7.94 (m, 2H), 7.88 (td, J = 7.8, 1.8 Hz, 1H), 7.41–7.38 (m, 1H), 7.36–7.33 (m, 2H), 7.26–7.23 (m, 3H), 3.19 (t, 2H, J = 7.4 Hz), 2.69 (t, 2H, J = 7.7 Hz), 1.86 (m, 2H), 1.72 (m, 2H), 1.53–1.44 (m, 4H); ^{13}C NMR (125 MHz, CDCl_3) δ 188.3, 157.3, 153.1, 150.0, 146.2, 142.6, 137.0, 128.3 (2C), 128.1 (2C), 126.8, 125.5, 124.0, 120.3, 39.0, 35.8, 31.2, 28.9 (2C), 23.8; IR (film) ν_{max} 3060, 3025, 2929, 2855, 1694, 1603, 1575, 1505, 1470, 1455, 1426, 1382, 1283, 1151, 1031, 990, 963, 936, 784, 741, 699 cm^{-1} ; MALDI-FTMS m/z 335.1756 ($\text{M} + \text{H}^+$, $\text{C}_{21}\text{H}_{22}\text{N}_2\text{O}_2$ requires 335.1754). Anal. ($\text{C}_{21}\text{H}_{22}\text{N}_2\text{O}_2$) C, H, N.

1-Hydroxy-1-[5-(2-pyridyl)oxazol-2-yl]-7-phenylheptane (23)

NaBH_4 (3 mg, 0.08 mmol) was added to a solution of **11f** (16 mg, 0.048 mmol) in a 1:1 mixture of MeOH and THF (0.5 mL). After stirring at 0 °C for 30 min, the reaction was quenched with the addition of saturated aqueous NaCl. The mixture was concentrated and extracted with EtOAc. The organic layers were combined, dried (Na_2SO_4), and concentrated.

Chromatography (SiO_2 , 1 × 4 cm, 35% EtOAc-hexanes) afforded **23** (13 mg, 0.039 mmol, 81%) as a pale yellow oil: ^1H NMR (400 MHz, CDCl_3) δ 8.62 (app d, 1H, J = 4.4 Hz), 7.75 (td, 1H, J = 7.7, 1.7 Hz), 7.64–7.62 (m, 2H), 7.28–7.14 (m, 6H), 4.87 (app t, 1H, J = 6.6 Hz), 3.42 (br s, 1H), 2.59 (app t, 2H, J = 7.6 Hz), 2.05–1.93 (m, 2H), 1.64–1.33 (m, 8H); ^{13}C NMR (125 MHz, CDCl_3) δ 167.2, 152.1, 149.8, 147.1, 142.7, 136.9, 128.3 (2C), 128.2 (2C), 125.5, 125.0, 123.0, 119.3, 67.7, 35.9, 35.5, 31.4, 29.1 (2C), 25.0; IR (film) ν_{max} 3284, 3025, 2929, 2855, 1614, 1580, 1547, 1471, 1427, 1117, 1074, 990, 950, 783, 743, 699 cm^{-1} ; MALDI-FTMS m/z 337.1911 ($\text{M} + \text{H}^+$, $\text{C}_{21}\text{H}_{24}\text{N}_2\text{O}_2$ requires 337.1916). Anal. ($\text{C}_{21}\text{H}_{24}\text{N}_2\text{O}_2$) C, H, N.

FAAH Inhibition

^{14}C -labeled oleamide was prepared from ^{14}C -labeled oleic acid as described.^{2,29} The truncated rat FAAH (rFAAH) was expressed in *E. coli* and purified as described.⁵⁰ The purified recombinant rFAAH was used in the inhibition assays unless otherwise indicated. The full-length human FAAH (hFAAH) was expressed in COS-7 cells as described¹⁴ and the lysate of hFAAH-transfected COS-7 cells was used in the inhibition assays where explicitly indicated.

The inhibition assays were performed as described.^{2,29} In brief, the enzyme reaction was initiated by mixing 1 nM of rFAAH (800, 500, or 200 pM rFAAH for inhibitors with $K_i \leq 1$ –2 nM) with 10 μM of ^{14}C -labeled oleamide in 500 μL of reaction buffer (125 mM TrisCl, 1

mM EDTA, 0.2% glycerol, 0.02% Triton X-100, 0.4 mM Hepes, pH 9.0) at room temperature in the presence of three different concentrations of inhibitor. The enzyme reaction was terminated by transferring 20 μ L of the reaction mixture to 500 μ L of 0.1 N HCl at three different time points. The 14 C-labeled oleamide (substrate) and oleic acid (product) were extracted with EtOAc and analyzed by TLC as detailed.^{2,29} The K_i of the inhibitor was calculated using a Dixon plot as described.⁴⁰ Lineweaver–Burk analysis was performed as described,^{29,40} in the presence or absence of 8 nM of **9f** or **11f**, respectively, confirming competitive, reversible inhibition (see Figure 2).

Selectivity Screening

The selectivity screening was conducted as detailed.⁴²

Computational Details

Cartesian coordinates for the 2.8 Å fatty acid amide hydrolase (FAAH) crystal structure complexed to methoxyarachidonyl phosphonate (MAP) (Brookhaven Protein Data Bank code: 1MT5) were employed.²² From the dimeric enzyme, only one active site was retained and taken as the center of the reacting system. Residues with any atom within 15 Å from the center of the reacting system were retained in the simulations and any clipped residues were capped with acetyl and *N*-methylamine groups. The MAP inhibitor was removed from the active site. Using the BOMB program,⁵¹ the inhibitors **9f** and **11f** were inserted and subsequently covalently bound to Ser241 in separate simulations. The enzymatic system then had 2677 atoms, consisting of 167 amino acid residues in addition to the inhibitors. Degrees of freedom for the protein backbone atoms were not sampled. Only side chains of residues with any atom within 10 Å from the center of the solute were varied. Partial atomic charges totaling -1 e were computed for the inhibitors **9f** and **11f** covalently bound to Ser241 using the CM1A model.⁵² Charge neutrality was then imposed by having a total protein charge of $+1$ e; charged residues near the active site were assigned normal protonation states at physiological pH, and the adjustments for neutrality were made to the most distant residues. The entire system was solvated with a 22-Å radius water cap consisting of 603 molecules for **9f** and 622 for **11f**, and a half-harmonic potential with a force constant of 1.5 kcal/mol·Å² was applied to water molecules at distances greater than 22 Å from the center of the solute to avoid evaporation.

Geometry optimizations for the enzyme covalently bound to the inhibitors were performed followed by MC statistical mechanics at 25 °C. Initial reorganization of the solvent was performed for 5×10^6 configurations. This was followed by 10×10^6 configurations of full equilibration and 50×10^6 configurations of averaging for each simulation. Established procedures including Metropolis and preferential sampling⁵³ were employed using the MCPRO 1.68 program.⁵⁴ The protein was represented with the OPLS-AA force field,⁵⁵ the TIP4P model⁵⁶ was used for water, and residue-based cutoffs of 10 Å were employed for all non-bonded solute-solute and solvent-solute interactions.

Supplementary Material

Refer to Web version on PubMed Central for supplementary material.

Acknowledgements

We gratefully acknowledge the financial support of the National Institutes of Health (DA15648, D.L.B.; DA13173, DA17259, and DA15197, B.F.C.; GM032136, W.L.J.) and the Skaggs Institute for Chemical Biology, fellowships for R.A.F. (American Cancer Society), and the postdoctoral sabbatical leave of H.M. sponsored by Sumitomo Pharmaceutical.

References

1. Dervane WA, Hanus L, Breuer A, Pertwee RG, Stevenson LA, Griffin G, Gibson D, Mandelbaum A, Etinger A, Mechoulam R. Isolation and structure of a brain constituent that binds to the cannabinoid receptor. *Science* 1992;258:1946–1949. [PubMed: 1470919]
2. Cravatt BF, Prospero-Garcia O, Suizdak G, Gilula NB, Henriksen SJ, Boger DL, Lerner RA. Chemical characterization of a family of brain lipids that induce sleep. *Science* 1995;268:1506–1509. [PubMed: 7770779]
3. Cravatt BF, Lerner RA, Boger DL. Structure determination of an endogenous sleep-inducing lipid, cis-9-octadecenamide (oleamide): a synthetic approach to the chemical analysis of trace quantities of a natural product. *J Am Chem Soc* 1996;118:580–590.
4. Boger DL, Henriksen SJ, Cravatt BF. Oleamide: an endogenous sleep-inducing lipid and prototypical member of a new class of biological signaling molecules. *Curr Pharm Des* 1998;4:303–314. [PubMed: 10197045]
5. Schmid HHO, Schmid PC, Natarajan V. N-acylated glycerophospholipids and their derivatives. *Prog Lipid Res* 1990;29:1–43. [PubMed: 2087478]
6. Martin BR, Mechoulam R, Razdan RK. Discovery and characterization of endogenous cannabinoids. *Life Sci* 1999;65:573–595. [PubMed: 10462059]
7. Di Marzo V, Bisogno T, De Petrocellis L, Melck D, Martin BR. Cannabimimetic fatty acid derivatives: the anandamide family and other “endocannabinoids”. *Curr Med Chem* 1999;6:721–744. [PubMed: 10469888]
8. Axelrod J, Felder CC. Cannabinoid receptors and their endogenous agonist, anandamide. *Neurochem Res* 1998;23:575–581. [PubMed: 9566594]
9. Zygmunt PM, Petersson J, Andersson DA, Chuang H, Sorgard M, Di Marzo V, Julius D, Hogestatt ED. Vanilloid receptors on sensory nerves mediate the vasodilator action of anandamide. *Nature (London)* 1999;400:452–457. [PubMed: 10440374]
10. Smart D, Gunthorpe MJ, Jerman JC, Nasir S, Gray J, Muir AI, Chambers JK, Randall AD, Davis JB. The endogenous lipid anandamide is a full agonist at the human vanilloid receptor (hVR1). *Br J Pharmacol* 2000;129:227–230. [PubMed: 10694225]
11. Walker JM, Huang SM, Strangman NM, Tsou K, Sanudo-Pena MC. Pain modulation by release of the endogenous cannabinoid anandamide. *Proc Natl Acad Sci USA* 1999;96:12198–12203. [PubMed: 10518599]
12. Huitron-Resendiz S, Gombart L, Cravatt BF, Henriksen SJ. Effect of Oleamide on sleep and its relationship to blood pressure, body temperature, and locomotor activity in rats. *Exp Neurology* 2001;172:235–243.
13. Cravatt BF, Giang DK, Mayfield SP, Boger DL, Lerner RA, Gilula NB. Molecular characterization of an enzyme that degrades neuromodulatory fatty-acid amides. *Nature (London)* 1996;384:83–87. [PubMed: 8900284]
14. Giang DK, Cravatt BF. Molecular characterization of human and mouse fatty acid amide hydrolases. *Proc Natl Acad Sci USA* 1997;94:2238–2242. [PubMed: 9122178]
15. Patricelli MP, Cravatt BF. Proteins regulating the biosynthesis and inactivation of neuromodulatory fatty acid amides. *Vit Hormones* 2001;62:95–131.
16. Boger DL, Fecik RA, Patterson JE, Miyauchi H, Patricelli MP, Cravatt BF. Fatty acid amide hydrolase substrate specificity. *Bioorg Med Chem Lett* 2000;10:2613–2616. [PubMed: 11128635]
17. Lang W, Qin C, Lin S, Khanolkar AD, Goutopoulos A, Fan P, Abouzid K, Meng Z, Biegel D, Makriyannis A. Substrate specificity and stereoselectivity of rat brain microsomal anandamide amidohydrolase. *J Med Chem* 1999;42:896–902. [PubMed: 10072686]
18. Egertova M, Cravatt BF, Elphick MR. Comparative analysis of fatty acid amide hydrolase and CB1 cannabinoid receptor expression in the mouse brain: evidence of a widespread role for fatty acid amide hydrolase in regulation of endocannabinoid signaling. *Neuroscience* 2003;119:481–496. [PubMed: 12770562]
19. Patricelli MP, Lovato MA, Cravatt BF. Chemical and mutagenic investigations of fatty acid amide hydrolase: evidence for a family of serine hydrolases with distinct catalytic properties. *Biochemistry* 1999;38:9804–9812. [PubMed: 10433686]

20. Patricelli MP, Cravatt BF. Fatty acid amide hydrolase competitively degrades bioactive amides and esters through a nonconventional catalytic mechanism. *Biochemistry* 1999;38:14125–14130. [PubMed: 10571985]
21. Patricelli MP, Cravatt BF. Clarifying the catalytic roles of conserved residues in the amidase signature family. *J Biol Chem* 2000;275:19177–19184. [PubMed: 10764768]
22. Bracey MH, Hanson MA, Masuda KR, Stevens RC, Cravatt BF. Structural adaptations in a membrane enzyme that terminates endocannabinoid signaling. *Science* 2002;298:1793–1796. [PubMed: 12459591]
23. Cravatt BF, Demarest K, Patricelli MP, Bracey MH, Giang DK, Martin BK, Lichtman AH. Supersensitivity to anandamide and enhanced endogenous cannabinoid signaling in mice lacking fatty acid amide hydrolase. *Proc Natl Acad Sci USA* 2001;98:9371–9376. [PubMed: 11470906]
24. Lichtman AH, Hawkins EG, Griffin G, Cravatt BF. Pharmacological activity of fatty acid amides is regulated, but not mediated, by fatty acid amide hydrolase in vivo. *J Pharmacol Exp Ther* 2002;302:73–79. [PubMed: 12065702]
25. Lichtman AH, Shelton CC, Advanti T, Cravatt BF. Mice lacking fatty acid amide hydrolase exhibit a cannabinoid receptor-mediated phenotypic hypoalgesia. *Pain* 2004;109:319–327. [PubMed: 15157693]
26. Cravatt BF, Lichtman AH. Fatty acid amide hydrolase: an emerging therapeutic target in the endocannabinoid system. *Curr Opin Chem Biol* 2003;7:469–475. [PubMed: 12941421]
27. Bisogno T, De Petrocellis L, Di Marzo V. Fatty acid amide hydrolase, an enzyme with many bioactive substrates. Possible therapeutic implications. *Curr Pharm Des* 2002;8:533–547. [PubMed: 11945157]
28. Fowler CJ, Jonsson K-O, Tiger G. Fatty acid amide hydrolase: biochemistry, pharmacology, and therapeutic possibilities for an enzyme hydrolyzing anandamide, 2-arachidonoylglycerol, palmitoylethanolamide, and oleamide. *Biochem Pharmacol* 2001;62:517–526. [PubMed: 11585048]
29. Patricelli MP, Patterson JP, Boger DL, Cravatt BF. An endogenous sleep-inducing compound is a novel competitive inhibitor of fatty acid amide hydrolase. *Bioorg Med Chem Lett* 1998;8:613–618. [PubMed: 9871570]
30. Koutek B, Prestwich GD, Howlett AC, Chin SA, Salehani D, Akhavan N, Deutsch DG. Inhibitors of arachidonoyl ethanolamide hydrolysis. *J Biol Chem* 1994;269:22937–22940. [PubMed: 8083191]
31. Patterson JE, Ollmann IR, Cravatt BF, Boger DL, Wong C-H, Lerner RA. Inhibition of oleamide hydrolase catalyzed hydrolysis of the endogenous sleep-inducing lipid cis-9-octadecenamide. *J Am Chem Soc* 1996;118:5938–5945.
32. Boger DL, Sato H, Lerner AE, Austin BJ, Patterson JE, Patricelli MP, Cravatt BF. Trifluoromethyl ketone inhibitors of fatty acid amide hydrolase: a probe of structural and conformational features contributing to inhibition. *Bioorg Med Chem Lett* 1999;9:265–270. [PubMed: 10021942]
33. Deutsch DG, Lin S, Hill WAG, Morse KL, Salehani D, Arreaza G, Omeir RL, Makriyannis A. Fatty acid sulfonyl fluorides inhibit anandamide metabolism and bind to the cannabinoid receptor. *Biochem Biophys Res Commun* 1997;231:217–221. [PubMed: 9070252]
34. Deutsch DG, Omeir R, Arreaza G, Salehani D, Prestwich GD, Huang Z, Howlett A. Methyl arachidonyl fluorophosphonate: a potent irreversible inhibitor of anandamide amidase. *Biochem Pharmacol* 1997;53:255–260. [PubMed: 9065728]
35. De Petrocellis L, Melck D, Ueda N, Maurelli S, Kurahashi Y, Yamamoto S, Marino G, Di Marzo V. Novel inhibitors of brain, neuronal, and basophilic anandamide amidohydrolase. *Biochem Biophys Res Commun* 1997;231:82–88. [PubMed: 9070224]
36. Fernando SR, Pertwee RG. Evidence that methyl arachidonyl fluorophosphonate is an irreversible cannabinoid receptor antagonist. *Br J Pharmacol* 1997;121:1716–1720. [PubMed: 9283708]
37. Edgemond WS, Greenberg MJ, McGinley PJ, Muthians S, Campbell WB, Hillard CJ. Synthesis and characterization of diazomethylarachidonyl ketone: an irreversible inhibitor of N-arachidonyl ethanolamine amidohydrolase. *J Pharmacol Exp Ther* 1998;286:184–190. [PubMed: 9655859]
38. Kathuria S, Gaetani S, Fegley D, Valino F, Duranti A, Tontini A, Mor M, Tarzia G, La Rana G, Calignano A, Giustino A, Tattoli M, Palmery M, Cuomo V, Piomelli D. Modulation of anxiety through blockade of anandamide hydrolysis. *Nature Med* 2003;9:76–81. [PubMed: 12461523]

39. Tarzia G, Duranti A, Tontini A, Piersanti G, Mor M, Rivara S, Plazzi PV, Park C, Kathuria S, Piomelli D. Design, synthesis, and structure–activity relationships of alkylcarbamic acid aryl esters, a new class of fatty acid amide hydrolase inhibitors. *J Med Chem* 2003;46:2352–2360. [PubMed: 12773040]
40. Boger DL, Sato H, Lerner AE, Hedrick MP, Fecik RA, Miyauchi H, Wilkie GD, Austin BJ, Patricelli MP, Cravatt BF. Exceptionally potent inhibitors of fatty acid amide hydrolase: the enzyme responsible for degradation of endogenous oleamide and anandamide. *Proc Natl Acad Sci USA* 2000;97:5044–5049. [PubMed: 10805767]
41. Boger DL, Miyauchi H, Hedrick MP. α -Keto heterocycle inhibitors of fatty acid amide hydrolase: carbonyl group modification and α -substitution. *Bioorg Med Chem Lett* 2001;11:1517–1520. [PubMed: 11412972]
42. Leung D, Hardouin C, Boger DL, Cravatt BF. Discovering potent and selective reversible inhibitors of enzymes in complex proteomes. *Nature Biotech* 2003;21:687–691.
43. Lichtman AH, Leung D, Shelton CC, Saghatelian A, Hardouin C, Boger DL, Cravatt BF. Reversible inhibitors of fatty acid amide hydrolase that promote analgesia: evidence for an unprecedented combination of potency and selectivity. *J Pharmacol Exp Ther*. in press
44. Harn NK, Gramer CJ, Anderson BA. Acylation of oxazoles by the copper-mediated reaction of oxazol-2-ylzinc chloride derivatives. *Tetrahedron Lett* 1995;36:9453–9456.
45. Nahm S, Weinreb SM. N-Methoxy-N-methylamides as effective acylating agents. *Tetrahedron Lett* 1981;22:3815–3818.
46. Farina V, Krishnamurthy V, Scott WJ. The Stille reaction. *Org React* 1997;50:1–652.
47. Dess DB, Martin JC. A useful 12-I-5 triacetoxypentadiene (the Dess–Martin periodinane) for the selective oxidation of primary or secondary alcohols and a variety of related 12-I-5 species. *J Am Chem Soc* 1991;113:7277–7287.
48. Vedejs E, Monahan SD. Metalation of oxazole–borane complexes: a practical solution to the problem of electrocyclic ring opening of 2-lithiooxazoles. *J Org Chem* 1996;61:5192–5193.
49. Hari Y, Obika S, Sakaki M, Morio K, Yamagata Y, Imanishi T. Effective synthesis of C-nucleosides with 2',4'-BNA modification. *Tetrahedron* 2002;58:3051–3063.
50. Patricelli MP, Lashuel HA, Giang DK, Kelly JW, Cravatt BF. Comparative characterization of a wild type and transmembrane domain-deleted fatty acid amide hydrolase: identification of the transmembrane domain as a site for oligomerization. *Biochemistry* 1998;37:15177–15187. [PubMed: 9790682]
51. Jorgensen, WL. BOMB, Version 2.4. Yale University; New Haven, CT: 2003.
52. Storer JW, Giesen DJ, Cramer CJ, Truhlar DG. Class-IV charge models – A new semiempirical approach in quantum chemistry. *J Comput-Aided Mol Design* 1995;9:87–110.
53. Allen, MP.; Tildesley, DJ. Computer Simulations of Liquids. Clarendon Press; Oxford, U K: 1987.
54. Jorgensen, WL. MCPRO, Version 1.68. Yale University; New Haven, CT: 2003.
55. Jorgensen WL, Maxwell DS, Tirado-Rives J. Development and testing of the OPLS allatom force field on conformational energetics and properties of organic liquids. *J Am Chem Soc* 1996;118:11225–11236.
56. Jorgensen WL, Chandrasekhar J, Madura JD, Impey W, Klein ML. Comparison of simple potential functions for simulating liquid water. *J Chem Phys* 1983;79:926–935.

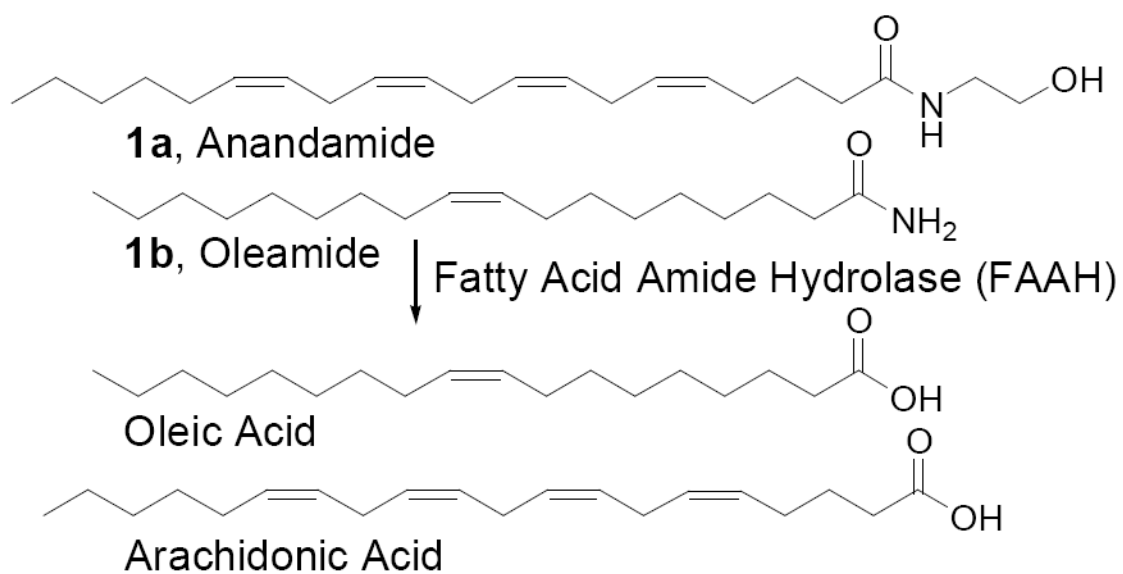


Figure 1.
FAAH substrates.

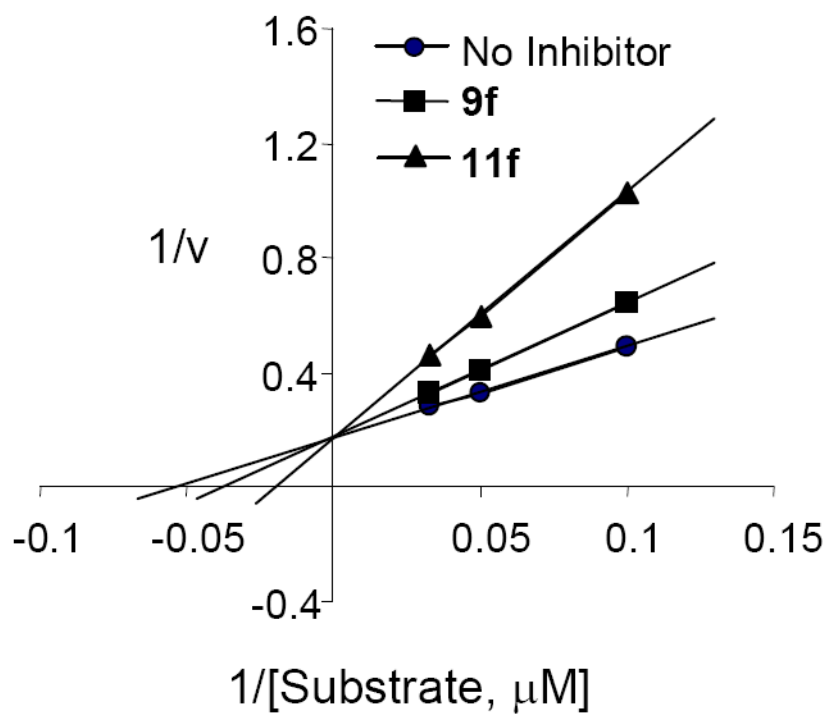


Figure 2. Lineweaver-Burk plot of FAAH inhibition by **9f** and **11f** illustrating reversible, competitive inhibition.

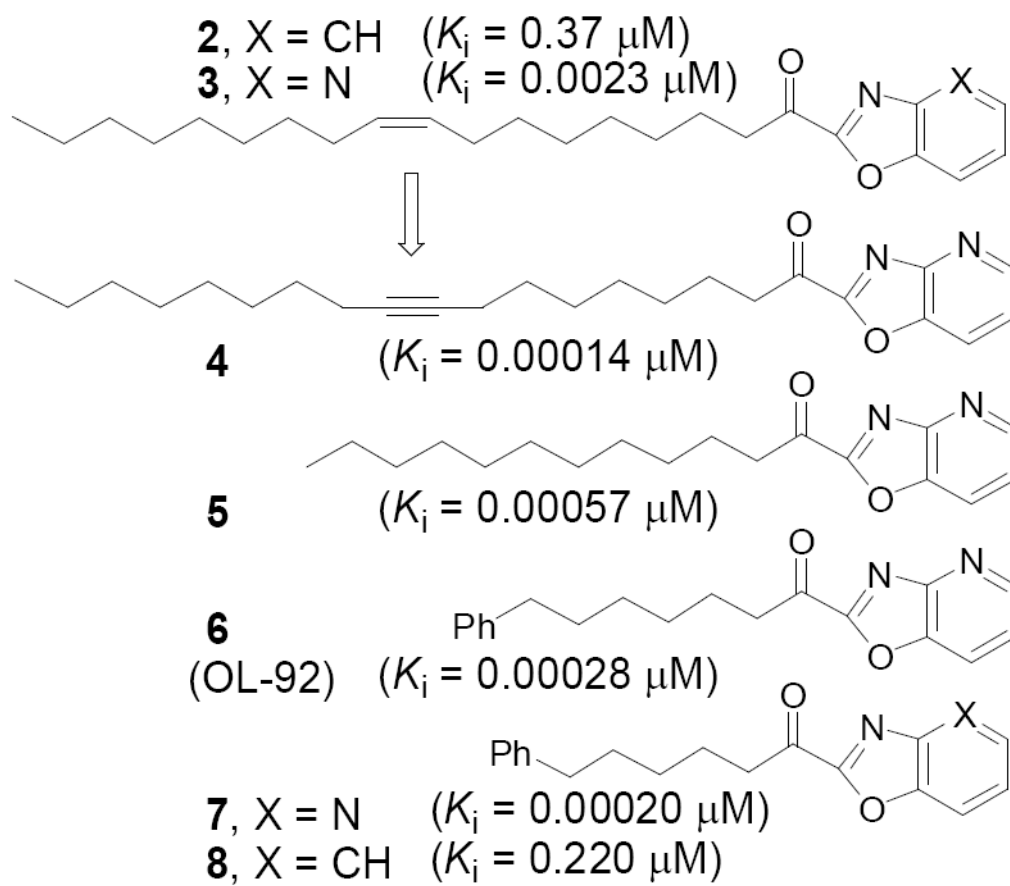


Figure 3.
 α -Keto oxazolopyridine FAAH inhibitors.⁴⁰

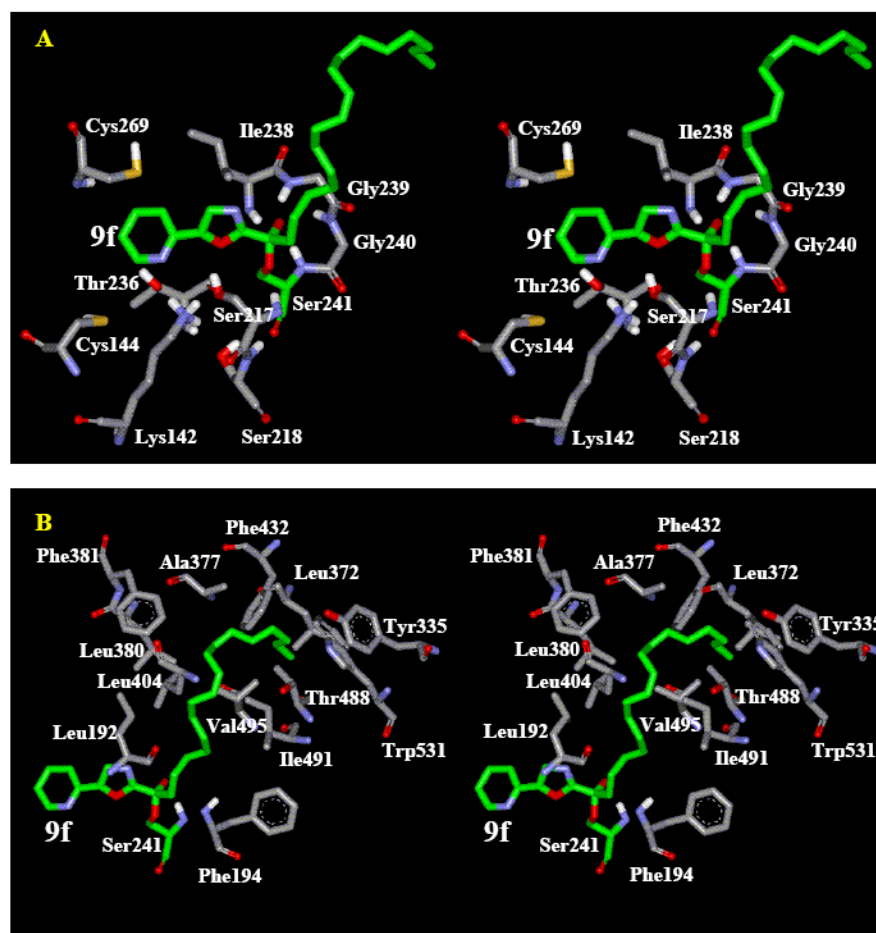
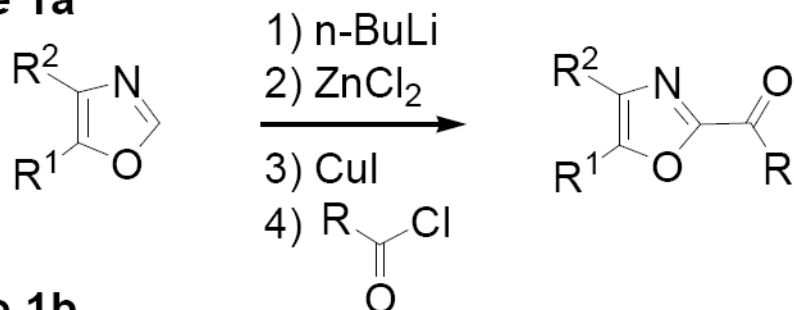
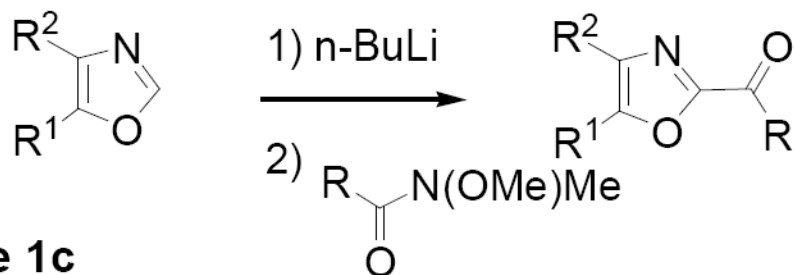
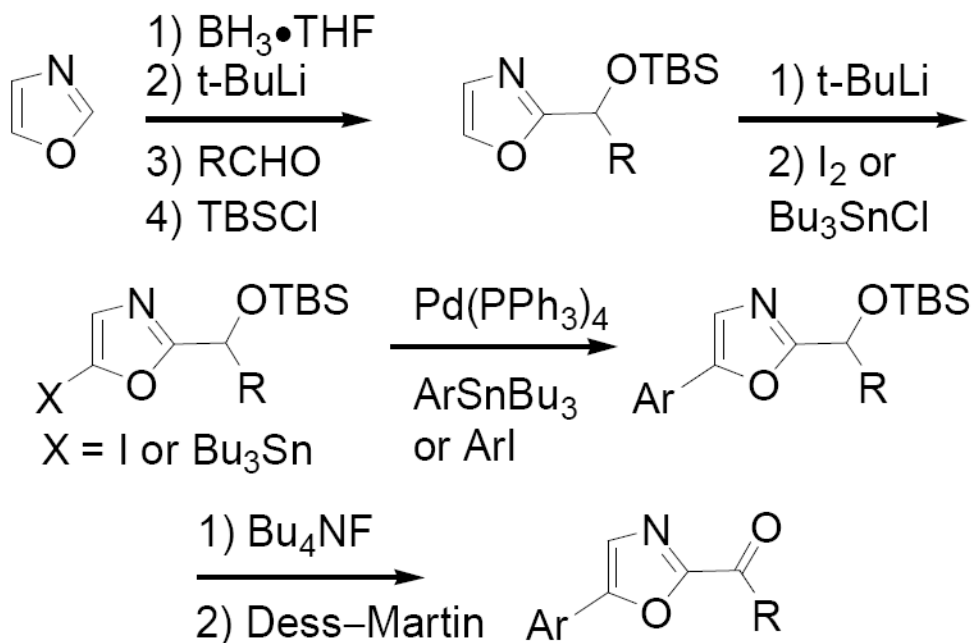


Figure 4.

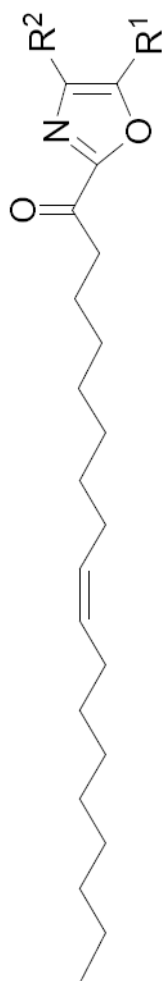
Stereo views of a snapshot from a MC simulation illustrating the interactions between **9f** and FAAH. (a) The extensive hydrogen-bonded network between the pyridyl-substituted oxazole ring and the enzyme, and interactions for the oxyanion (similar interactions occur for **11f**). (b) Interactions of the lipid chain of **9f** with hydrophobic residues in the active site.

Scheme 1a**Scheme 1b****Scheme 1c**

Scheme 1.

Table 1

Substituted α -Keto Oxazole Inhibitors of FAAH



compd	R ¹ /R ²	K _i , μ M	compd	R ¹ /R ²	K _i , μ M
9a	H/H	0.10 \pm 0.06	9b	Me/Me	3.8 \pm 0.2
9c	Ph/Ph	> 100	compd	R ²	K _i , μ M
9d		0.32 \pm 0.05	9e		0.49 \pm 0.03
9f		0.018 \pm 0.005	9g		0.031 \pm 0.006
9h		0.061 \pm 0.004	9i		0.041 \pm 0.010
9j		N 0.056 \pm 0.003	9k		0.078 \pm 0.014
compd	R ¹	K _i , μ M	compd	R ¹	K _i , μ M
9l		0.014 \pm 0.001	9m		0.016 \pm 0.001
9n		0.018 \pm 0.001	9o		0.016 \pm 0.001

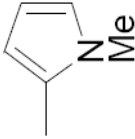
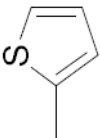
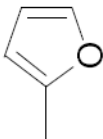
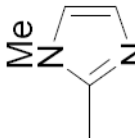
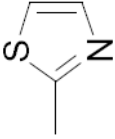
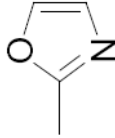
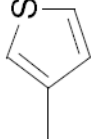
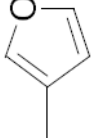
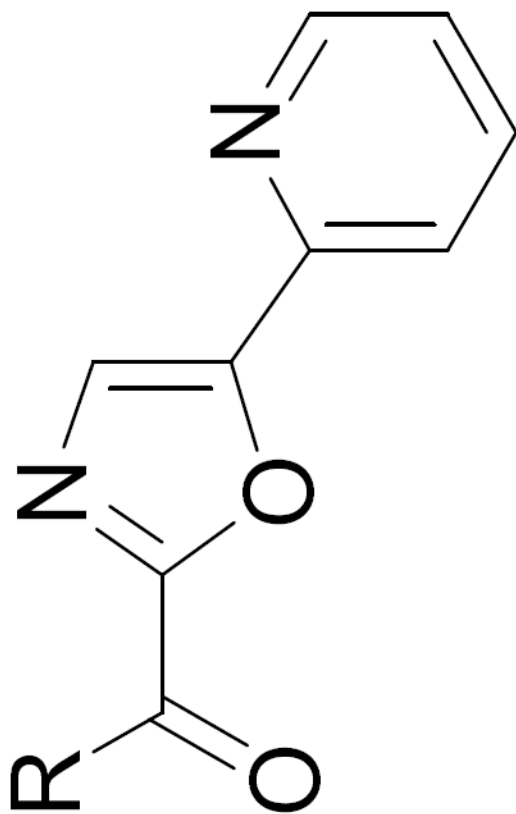
compd	R^1/R^2	K_i , μM	compd	R^1/R^2	K_i , μM
9p		8.6 \pm 2.1	9q		0.89 \pm 0.03
9r		0.054 \pm 0.004	9s		0.047 \pm 0.006
9t		0.016 \pm 0.002	9u		0.012 \pm 0.001
9v		13.2 \pm 4.1	9w		0.61 \pm 0.09

Table 2

Modifications in the Fatty Acid Side Chain^a

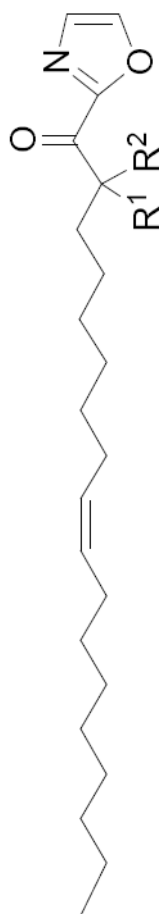


compd	R	K _i , μM	compd	R	K _i , μM
10a	CH ₃ (CH ₂) ₁₆	0.059	11a	Ph(CH ₂) ₁	17
10b	CH ₃ (CH ₂) ₁₄	0.021	11b	Ph(CH ₂) ₂	0.20
10c	CH ₃ (CH ₂) ₁₂	0.013	11c	Ph(CH ₂) ₃	0.12
10d	CH ₃ (CH ₂) ₁₀	0.0022	11d	Ph(CH ₂) ₄	0.033
10e	CH ₃ (CH ₂) ₉	0.0033	11e	Ph(CH ₂) ₅	0.011
10f	CH ₃ (CH ₂) ₈	0.0090	11f	Ph(CH ₂) ₆	0.0047
10g	CH ₃ (CH ₂) ₇	0.015	11g	Ph(CH ₂) ₇	0.0075
10h	CH ₃ (CH ₂) ₆	0.049	11h	Ph(CH ₂) ₈	0.0078
10i	CH ₃ (CH ₂) ₅	0.17	11i	Ph(CH ₂) ₉	0.010
10j	CH ₃ (CH ₂) ₄	0.94	11j	Ph(CH ₂) ₁₀	0.022
10k	CH ₃ (CH ₂) ₃	3.0			
10l	CH ₃ (CH ₂) ₂	11			
10m	CH ₃ CH ₂	48			
10n	CH ₃	>100			
12					0.010
13	CH ₂ =CH(CH ₂) ₇	0.011		14	HC=C(CH ₂) ₇
15	HC=CH(CH ₂) ₄	1.3		16	TMSC-C(CH ₂) ₄
17	PhC=CH(CH ₂) ₄	0.020		18	PhC=CH(CH ₂) ₃

^aMeasurement errors (±) are provided in Supporting Information

Table 3

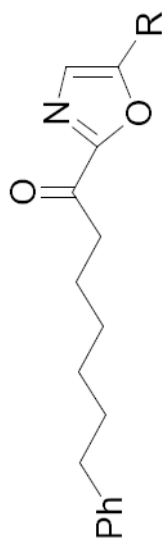
Effect of α -Substitution



compd	R^1/R^2	K_p μ M	compd	R^1/R^2	K_p μ M
19a	H/Me	1.4 \pm 0.1	19b	Me/Me	14.2 \pm 1.1

Table 4

Heteroaromatic Modifications to **11f**^a

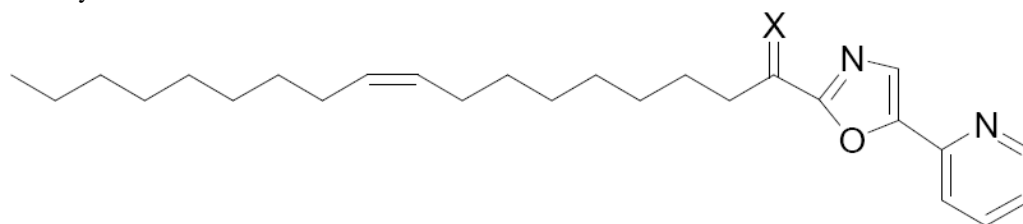


compd	R	K_i , μ M	compd	R	K_i , μ M
20a		0.14	20b		0.0056
20c		0.0023	20d		0.0053
20e		0.0046	20f		0.022
20g		0.055	20h		0.012
20i		0.0058	20j		0.0046

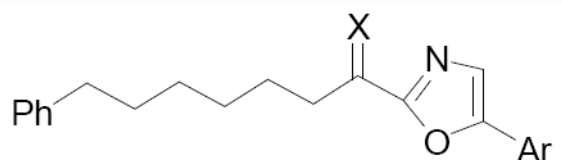
^a Measurement errors (\pm) are provided in Supporting Information

Table 5

Carbonyl Role



compd	X	K_i , μM
9f	O	0.018 ± 0.005
21	H,OH	10.6 ± 2.8
22	H,H	23.2 ± 6.3



compd	Ar	X	K_i , μM
11f		O	0.0047 ± 0.0013
23		H,OH	3.3 ± 0.3
24		H,H	20 ± 1
20b		O	0.0056 ± 0.0003
25		H,OH	4.3 ± 0.01
20e		O	0.0046 ± 0.0001
26		H,OH	5.9 ± 0.2

Table 6
Inhibition of Recombinant Human Fatty Acid Amide Hydrolase (FAAH)

compd	K_i , μM (human)	K_i , μM (rat)
9a	0.045 ± 0.002	0.10 ± 0.06
9f	0.010 ± 0.001	0.018 ± 0.005
11f	0.0090 ± 0.0001	0.0047 ± 0.0013

Table 7Selectivity Screening: IC₅₀, μM (selectivity)

	K_i (FAAH, mM)	$\text{CH}_3(\text{CH}_2)_7\text{CH}=\text{CH}(\text{CH}_2)_7\text{COCF}_3$ FAAH	KIAA	TGH
	0.08	4.5	1.1 (0.25)	4.8 (1.1)
n	K_i (FAAH, mM)	$\text{CH}_3(\text{CH}_2)_n\text{COCF}_3$ FAAH	KIAA	TGH
6	1.2	30	1.5 (0.05)	0.002 (0.00007)
8	0.13	10	0.4 (0.04)	0.01 (0.001)
10	0.14	10	0.5 (0.05)	0.06 (0.006)
16	0.24	6.4	6.6 (1)	4.6 (0.7)
n	K_i (FAAH, mM)	$\text{Ph}(\text{CH}_2)_n\text{COCF}_3$ FAAH	KIAA	TGH
0	nd	>100	10 (<0.10)	0.004 (<0.00004)
1	nd	>100	100 (<1)	0.010 (<0.0001)
5	0.17	5	0.8 (0.16)	0.0005 (0.0001)
6	0.10	5	0.2 (0.04)	0.001 (0.0002)
7	0.025	2	0.2 (0.1)	0.005 (0.002)
compd	K_i (FAAH)	representative α -ketoheterocycles ^a FAAH KIAA		TGH
2	0.37	10	>100 (>10)	10 (1)
9a	0.10	2	>100 (>50)	9 (4)
3	0.0023	0.04	60 (1500)	1 (25)
9f	0.018	0.15	>100 (>670)	>100 (>670)
8	0.22	10	>100 (>10)	0.02 (0.002)
7	0.00020	0.001	10 (10000)	0.001 (1)
6	0.00028	0.0003	20 (67000)	0.003 (10)
11f	0.0047	0.002	>100 (>10000)	0.6 (300)
4	0.00014	0.002	20 (10000)	0.5 (250)
12	0.01	0.02	>100 (>2000)	30 (1500)

^a Full table of results is provided in the Supporting Information